



HAL
open science

Design and Experimental Study of Intensifier for Deep Geothermal Drilling

Yuhang He, Hualin Liao, Hedi Sellami, John-Paul Latham, Jiansheng Xiang,
Laurent Gerbaud

► **To cite this version:**

Yuhang He, Hualin Liao, Hedi Sellami, John-Paul Latham, Jiansheng Xiang, et al.. Design and Experimental Study of Intensifier for Deep Geothermal Drilling. World Geothermal Congress, Sep 2023, BeiJing, China. hal-04437361

HAL Id: hal-04437361

<https://hal.science/hal-04437361>

Submitted on 4 Feb 2024

HAL is a multi-disciplinary open access archive for the deposit and dissemination of scientific research documents, whether they are published or not. The documents may come from teaching and research institutions in France or abroad, or from public or private research centers.

L'archive ouverte pluridisciplinaire **HAL**, est destinée au dépôt et à la diffusion de documents scientifiques de niveau recherche, publiés ou non, émanant des établissements d'enseignement et de recherche français ou étrangers, des laboratoires publics ou privés.

Design and Experimental Study of Intensifier for Deep Geothermal Drilling

Yuhang He^a; Hualin Liao^{a*}; Hedi Sellami^b; John-Paul Latham^c; Jiansheng Xiang^c; Laurent Gerbaud^b

a. School of Petroleum Engineering at China University of Petroleum (East China), Qingdao, 266580, China.

b. MINES ParisTech, PSL-Research University, Geosciences Research Center, Pau, 64000 Pau, France.

c. Earth Science and Engineering, Imperial College London, London, SW7 2AZ, United Kingdom.

E-mail address: liaohualin2003@126.com (Hualin Liao)

Keywords: Deep geothermal drilling; Intensifier; Output characteristics; CFD; Laboratory test

ABSTRACT

The rock of deep geothermal reservoir has the characteristics of high in-situ stress, high strength and high abrasiveness, which leads to slow ROP and low drilling efficiency during the drilling process of geothermal resource development. Ultra-high pressure jet slotting can effectively release local stress at the bottom-hole area and improve the rock-breaking ability during drilling. Therefore, in order to increase the pressure of the jet as much as possible and form an effective slotting at the bottom of the well, this paper designs an efficiently downhole intensifier device directly driven by the energy of the drilling mud. The parameters affecting the supercharging performance and stagnation pressure of the intensifier are analyzed by means of CFD simulation, and the output characteristics of the intensifier are tested by means of laboratory experiments. The results show that the greater the ratio of the input pressure to the piston area of the pressurizing chamber and the greater the output pressure, and the faster the working frequency of the intensifier. Increasing the stroke of the piston can prolong the holding time of the high-pressure water jet. Laboratory test results show that the output pressure waveform of the intensifier is square wave, and the area ratio of the supercharger chamber is approximately equal to its supercharger ratio. Compared with conventional geothermal drilling methods, the ultra-high pressure jet generated by the intensifier studied in this paper is coupled with the mechanical shock, which can provide a new deep geothermal drilling speed-up method and technology. So it can provide a theoretical and technical support for promoting the efficient and low-cost exploitation of geothermal resources.

1. INTRODUCTION

The green, clean and sustainable utilization of geothermal energy and the development of deep geothermal energy are the research hotspots and development trends in the world energy field^[1-4]. However, deep geothermal heat is mainly concentrated at the junction of plates^[5-6], which have the characteristics of high stress, high strength and high abrasiveness^[7-9]. In this paper, the speed-up idea of the coupling of ultra-high pressure water jet and mechanical shock is adopted, and the ultra-high pressure water jet is used to form cutting grooves on the bottom-hole rock surface, which can effectively release the local stress of the rock and reduce the difficulty of the bottom-hole drill bit in the process of mechanical shock drilling (as is shown in figure 1).

In order to realize the above concepts, strengthening the bottom-hole hydraulic energy is the key to realize the ultra-high pressure jet and mechanical coupling impact rock breaking. The US. Department of Energy (DOE), Flow drill and GRI cooperated to develop the second-generation downhole pump prototype, which increased the pressure of about 7% of a small part of the bottom hole fluid to 207MPa^[10-11]. The rock-breaking speed of the water jet is 1.45 times that of the conventional rock-breaking speed, which is the first application of the downhole booster device in the field of oil drilling^[12-13]. Since 1995, many types of intensifiers based upon various pressurizing modes have been developed, such as hydrostatic, diaphragm, centrifugal style, screw motor style, jet booster and so on. However, because of the complex intensifier structure and the short working life, seldom of them have been widely applied in oil and gas fields. Besides, the design principles of some intensifiers have certain shortcomings, which limit their applicability^[14-16].

The pressurizing performance and the characteristics of water jet distribution can significantly affect the efficiency of rock breaking; the deep geothermal drilling conditions are harsh. In order to further improve the pressurization capability and applicability of the downhole pressurization device, a new valve stem reversing type downhole pressurization device is proposed in this paper. therefore, based on the working principle of intensifier, firstly, the force of the plunger was analyzed and the nozzle pressure drop prediction model is derived by using the Bernoulli equation which ignores gravity. Secondly, the jet formation process, characteristic of water jet distribution and pressurization performance under different parameters were studied based on computational fluid dynamics (CFD). Finally, carrying out the intensifier prototype laboratory to verify the numerical simulation results.

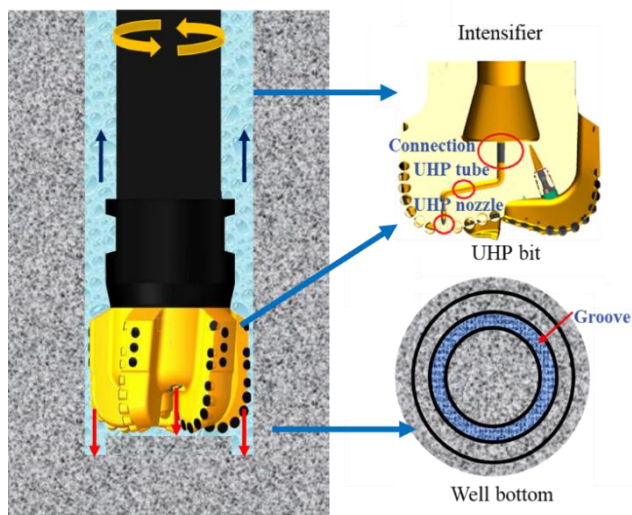


Figure 1 Schematic diagram of high-pressure water jet groove cutting

2. WORKING DESCRIPTION OF INTENSIFIER

The new valve stem intensifier is mainly composed of input flow channel, output flow channel, reversing guide rod, reversing block, plunger, stopper, one-way valve, high-pressure flow channel and so on. The outer diameter of the downhole intensifier is 220mm, and the piston area ratio of the intensifier is 1:5. During the working process of the device, there are mainly two states of the pressurization stroke and the reset stroke. During the pressurization process, the drilling fluid energy directly drives the pressurized piston. The fluid is pressurized, and the energy conversion efficiency is high. In addition, the pressurizing device has a simple structure, thereby improving the service life of the intensifier (as shown in figure 2).

Pressurization process: In initial state, the relieving flow channel was closed and the pressurizing flow channel was opened, the plunger is at the left-most end of the pressuring chamber. the rod reaches to the spacing device of the plunger, under the action of inertia, pushing the plunger and resetting valve move together until the resetting valve close the pressurizing flow channel and open the relieving flow channel closed, when the rod reaches to the spacing device of the plunger, under the action of inertia, pushing the plunger and resetting valve move together until the resetting valve opened the relieving flow channel and closed the pressurizing flow channel.

Reset process: At this state, the relieving flow channel was closed and pressurizing flow channel was opened, the plunger is at the left-most end of the pressuring chamber. part of working fluid enters the right of the chamber, the pressure on the left side of the one-way valve is greater than the pressure on the right side, one-way valve closed. the pressure at the left end of the plunger is the nozzle pressure drop, the pressure at the right end of the plunger is equal to the annular pressure, pushing the plunger move to the left, in this stage, the friction between plunger and connecting rod is less than that between connecting rod and damping block, the rod is fixed until it reaches to the spacing device of the plunger is reached .when the rod reaches to the spacing device of the plunger, under the action of inertia, pushing the plunger and resetting valve move together until the resetting valve close the relieving flow channel and open the pressurizing flow channel.

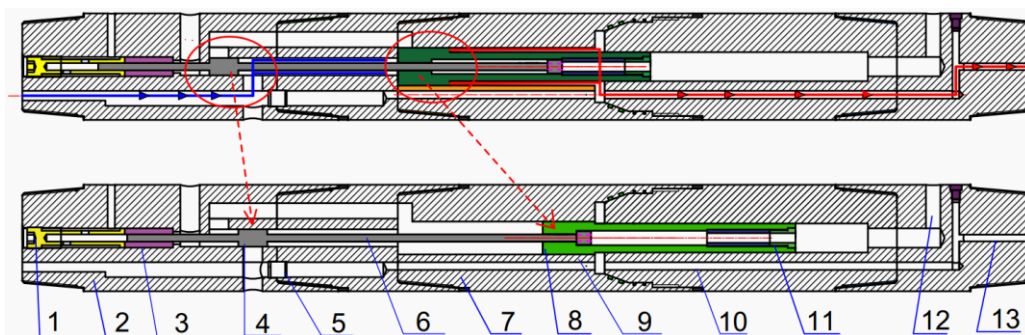


Figure 2 Schematic diagram of the new valve stem intensifier

3 OUTPUT PRESSURE ANALYSIS OF NEW INTENSIFIER

3.1 Force analysis of plunger

The plunger movement model of the intensifier is shown in Figure 3. The upper plunger is the low-pressure chamber, the lower plunger is a pressurizing chamber, the inlet is connected to a low-pressure chamber, and the outlet is connected to a high-pressure flow channel. The volume of fluid in the upper and lower chambers of the piston changes with the movement of the piston. The theoretical model of the supercharging cylinder is established according to the piston motion process equation.

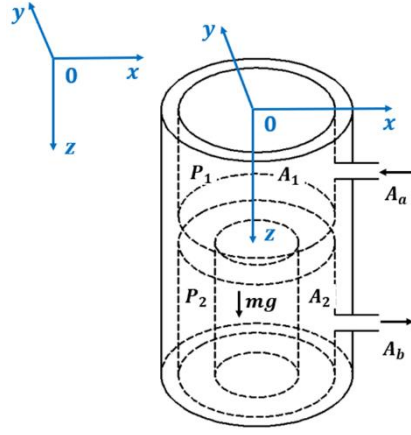


Figure 3 plunger movement model of the intensifier

According to the force analysis of the plunger during pressurization, the plunger motion equation can be obtained:

$$P_1 A_1 - P_2 A_2 = m a \quad (1)$$

Where P_1 is the pressure of low pressure chamber, MPa; A_1 is the effective area of the low-pressure chamber, m^2 ; P_2 is the pressure of booster chamber, MPa; A_2 is the effective area of the booster chamber, m^2 ;

Since the gravity of the piston in formula (1) is far less than the pressure on both ends of the piston, it can be ignored. Consider the acceleration as the second derivative of the displacement of the piston movement to the time:

$$P_1 A_1 - P_2 A_2 = m \frac{d^2 s}{dt^2} \quad (2)$$

Where S is the displacement of piston movement, m; T is the time of piston movement, s.

According to the orifice flow formula:

$$Q_2 = C_g A_b \sqrt{\frac{2\Delta P}{\rho}} \quad (3)$$

Where Q_2 is the flow of intensifier chamber, L/s ; C_g is the flow coefficient; $\Delta P = P_2 - P_0$, MPa; ρ is the density of the fluid, Kg/m^3 ; A_b is the sectional area of the outlet, m^2 .

According to the intensifier chamber flow conservation formula:

$$Q_2 = S_2 V_2 \quad (4)$$

Where: V_2 is the flow velocity of fluid in the pressurized chamber, m/s .

Regarding the speed v_2 as the first derivative of displacement to time, and formula (4) and formula (3) are combined to obtain:

$$S_2 \frac{ds}{dt} = C_g A_b \sqrt{\frac{2\Delta P}{\rho}} \quad (5)$$

Since the pressure P_0 is equal to bit pressure drop, which is far less than P_1 and P_2 , it can be ignored:

$$\frac{dv}{dt} + \frac{A_2^3 \rho}{2m C_g^2 A_b^2} \left(\frac{ds}{dt}\right)^2 = \frac{P_1 A_1}{m} \quad (6)$$

Where $k = \frac{A_2^3 \rho}{2m C_g^2 A_b^2}$; $b = \frac{P_1 A_1}{m}$, V is the speed of the piston, m/s .

3.2 Numerical simulation of the Intensifier

3.2.1 Finite element model of the intensifier chamber

In order to simplify the calculation, the following assumptions are adopted in this paper: 1. The pressurization chamber of the intensifier has good tightness and no leakage; 2. The contact between the piston cavity and the piston rod is smooth, that is, the influence of friction on the piston movement process is not considered; 3. Ignore the energy change generated by the fluid during the high-speed movement of the pressurized chamber.

The piston cavity fluid domain pressurization model is established according to the fluid flow mode in the intensifier pressurization stroke, as shown in figure 4. The dimensions of the fluid domain model are as follows: the initial liquid length is 10mm, the piston thickness is 60mm, the piston stroke is 500mm, the piston chamber diameter is 66mm, the piston rod diameter is 68mm, In order to improve the mesh quality, hexahedral structured mesh and O-type segmentation are used for mesh division, and interface matching is used between the boundaries of the fluid domain mesh for data transfer. Finally, the hexahedral structured mesh as shown in figure 4 is formed.

Table 1 Structural parameters of the intensifier chamber

| Parameters | Value |
|-------------------------|-------|
| Plunger diameter | 68mm |
| Plunger piston diameter | 60mm |
| Plunger stroke (Max) | 500mm |
| Nozzle diameter | 2mm |
| Input drilling pressure | 20MPa |

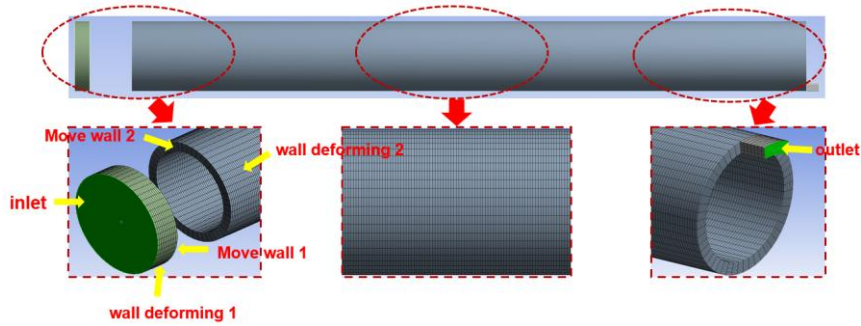


Figure 4 Physical model of numerical simulation

3.2.2 Piston motion grid control model

The movement of the piston will cause the shape of the piston cavity basin to change. This changed flow field is the basic form of the moving boundary flow field, so the dynamic grid technology needs to be applied. The influence of moving boundary movement should be considered when calculating the piston cavity basin by using the dynamic grid technology, and its motion equation expression is as follows:

$$\frac{d}{dt} \int_v \rho \Phi dV + \int_{\partial v} \rho \Phi (u - u_g) dA = \int_{\partial v} \Gamma \Delta \Phi dA + \int_v \rho \Phi dV \quad (7)$$

Where Φ is a general variable; v is the control volume, m^3 ; ρ is the liquid density, Kg / m^3 ; ∂v is the boundary of control volume; u_g is the moving speed of moving grid boundary, m / s ; u is the velocity vector, m / s ; S_Φ is the source item; Γ is the diffusion coefficient.

The movement of the piston in the booster chamber is mainly generated by the pressure at both ends of the piston and its own gravity. The acceleration at each moment is generated by the iteration of the last moment. The acceleration function in the n th iteration time step can be obtained as follows:

$$a^{(n)} = [\sum_{i=1}^m p_i^{(n-1)} a_i^{(n-1)} - \sum_{j=1}^n p_j^{(n-1)} a_j^{(n-1)}] / m - g \quad (8)$$

Where a_i and p_i is the area of the grid on the boundary of the piston near the low-pressure chamber, m^2 and pressure, MPa ; a_j and p_j is the area, m^2 and pressure, MPa , of the grid on the boundary of the piston near the intensifier chamber.

The velocity formula in the nth iteration time step is:

$$v^{(n)} = v^{(n-1)} + a^{(n)} \Delta T \tag{9}$$

Where ΔT is the iteration time step of each step, s .

3.3 Numerical simulation results

3.3.1 The feature of output UHP jet

According to the above finite element model, use Fluent software to analyze the high-pressure fluid output characteristics of the pressurized chamber, the feature of output ultrahigh pressure jet was shown as the figure 5.

Figure.5(a) shows the relationship between pressuring chamber pressure and time, With the movement of the piston during pressurization, the fluid pressure in the pressurization chamber rapidly reaches the peak pressure in a short time, and then the peak value of velocity maintain a continuous steady interval, when the input drilling pressure is 20Mpa, output peak value of pressure are about 97Mpa , at this time, the pressure at both ends of the piston reaches equilibrium, When the piston moves to the limit position of the stroke, the pressure in the booster chamber drops sharply,; Figure.5(b) shows the relationship between ultrahigh pressure jet speed and time, With the movement of the piston during pressurization, The fluid in the chamber pressuring was pressurized, the fluid velocity at the high-pressure outlet reaches the peak rapidly, high-speed jet was ejected through high-pressure nozzle and acts on the rock surface at the bottom of the well to form rock cutting groove at the bottom of the well. Figure.5(c) shows the relationship between piston movement speed and time, the liquid enters the upper chamber of the piston from the upper joint. Due to the difference in the area between the left and right sides of the piston, the piston is pushed to the right, the piston movement first reaches the peak speed in a short time, then the left and right pressures of the piston reach balance, and the piston presents a uniform motion state. When the piston reaches the limit position of the piston stroke, the piston stops moving, and the pressurization process ends.

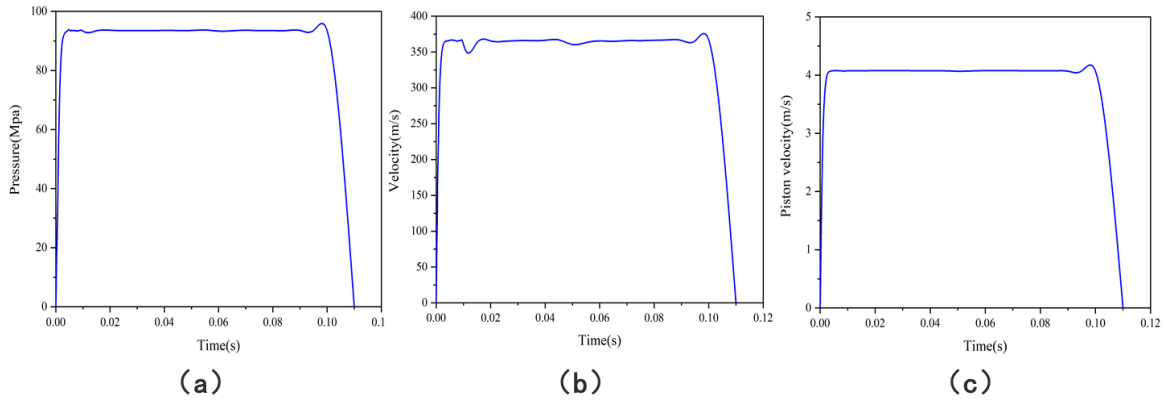


Figure 5 Output pressure characteristic curve

3.3.2 Characteristic of flow field

(a) Plunger Stroke

In the design process of intensifier, the movement stroke of piston affects the overall length of intensifier, Figure.6 shows the relationship between intensifier stroke and its output pressure characteristics. Take the stroke of the intensifier as 200mm, 300mm,500mm,700mm and 1000mm respectively to analyze the output characteristics of the pressurizing chamber. With the plunger stroke increase, the peak pressure of fluid and the ejection velocity of fluid in the pressurizing chamber are basically unchanged, but the movement period of the piston becomes longer and the peak pressure storage time becomes longer. The intensifier maintains a longer peak pressure, which is more conducive to the fracture of the bottom hole rock, thus forming an effective bottom hole stress notch, and realizing the local stress unloading of the bottom hole rock, So, it is more advantageous to increase the stroke of the intensifier when the design requirements allow.

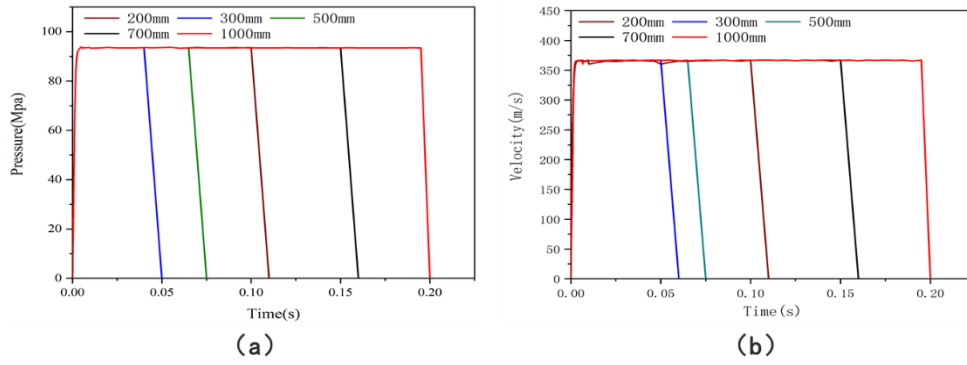


Figure 6 In different plunger stroke intensifier output pressure characteristic curve

(b) Area Ratio

During pressurization process of the intensifier, Due to the different piston area ratio on both sides of the pressurizing chamber, the hydraulic differential pressure force is generated to push the piston to move. Figure.7 shows the relationship between chamber area ratio and its output pressure characteristics. Under this condition, the input pressure of intensifier is 20MPa, take the area ratio of the intensifier as 1:3, 1:4, 1:4.5, 1:5 and 1:6 respectively to analyze the output characteristics of the pressurizing chamber, the ratio of pressurizing chamber output peak pressure to input pressure is basically equal to the piston area ratio. When the input pressure of the intensifier is the same, the larger the area ratio of the intensifier piston, the greater the output pressure of the intensifier. At this time, the faster the piston moves, the shorter the cycle of pressurizing stroke, and the faster the intensifier moves. Therefore, the piston area ratio should be increased as much as possible when designing the size of the pressurizing chamber, and the increase of the area ratio will also reduce the amount of fluid discharged from the pressurizing chamber. Therefore, the area ratio of the booster chamber piston should be increased under the condition that the output flow is met.

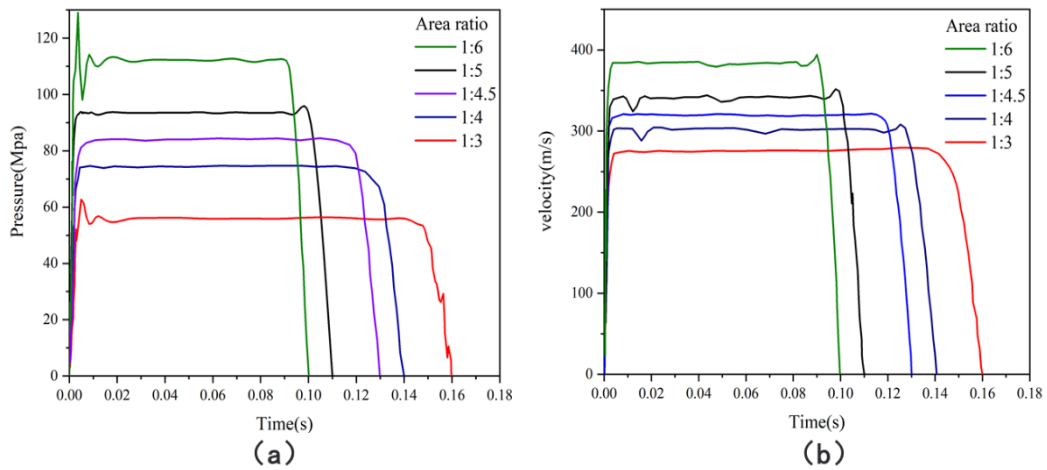


Figure 7 In different area ratio intensifier output pressure characteristic curve

(c) Input Pressure

The driving energy of the downhole intensifier designed in this paper comes from the drilling fluid energy, the drilling fluid energy directly acts on the left side of the piston, driving the piston in the pressurizing chamber to move to the right, making the fluid pressure in the pressurizing chamber increase. Figure.8 shows the relationship between chamber input pressure and its output pressure characteristics. In this condition, taking the input pressure of the intensifier as 10MPa, 15MPa, 20MPa, 25MPa and 30MPa respectively to analyze the output characteristics of the pressurizing chamber. The greater the input pressure and output pressure of the intensifier, the faster the piston movement speed and the faster the intensifier movement frequency. In order to further improve the output pressure of the intensifier, the input pressure of the intensifier should be increased as much as possible under the construction conditions during the field operation.

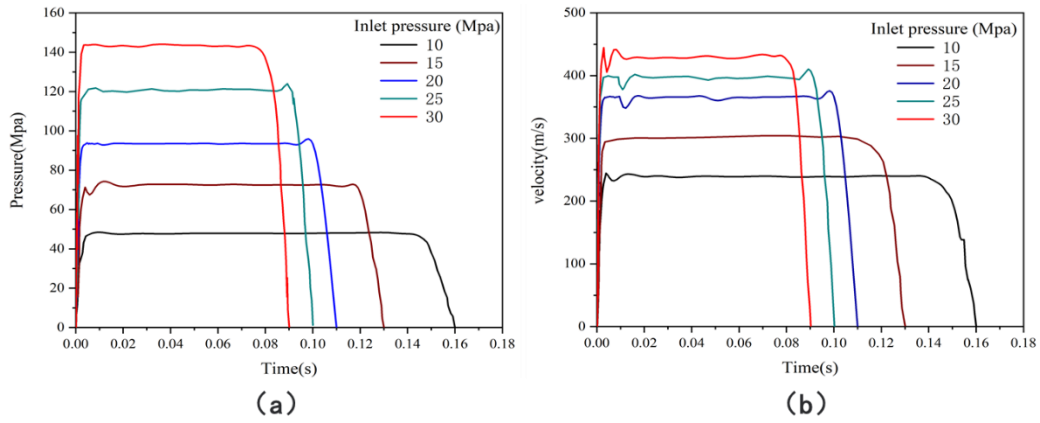


Figure 8 In different input pressure intensifier output pressure characteristic curve

4 INTENSIFIER PROTOTYPE LABORATORY TEST

In order to verify the correctness of the above theoretical analysis and numerical simulation results, the downhole intensifier prototype is processed, and the prototype functional test and output characteristic test are carried out. The schematic diagram of laboratory experiment is shown in figure 9, During the experiment, the inlet pressure is controlled by the pump pressure. Pressure sensors are installed at the left and right ends of the booster chamber to test the pressure change of the pressurizing chamber during the operation of the pressurizing process. To simplify the experiment, the channels were externally connected.

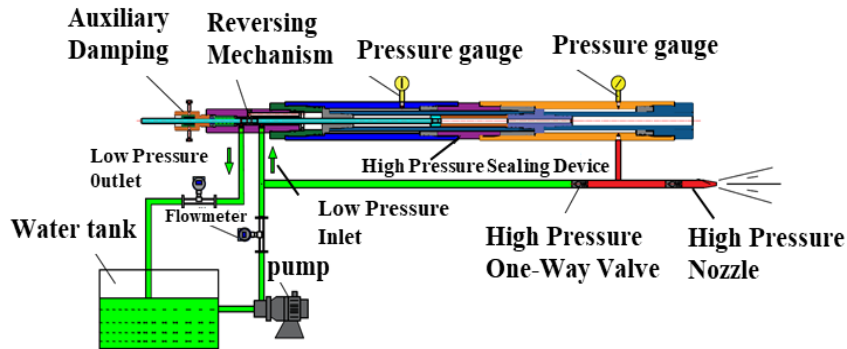


Figure 9 Schematic diagram of intensifier laboratory test

The parameters of the intensifier prototype are as follows: the diameter of pressurizing chamber is 77mm, the diameter of piston rod is 68mm, the area ratio of plunger is about 1:4.54. In order to ensure the safety of the experiment, the low pressure inlet is used to test the output characteristic of the intensifier. The inlet pressure is 2MPa and 3.5MPa respectively to test the output characteristic curve of the supercharger, as is shown in figure 10.

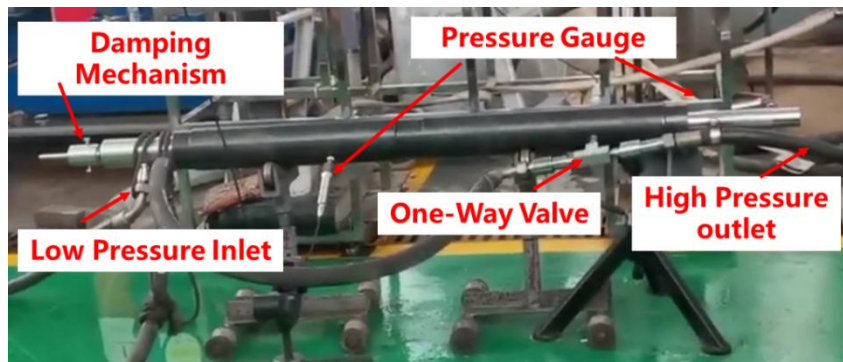


Figure.10 Laboratory test diagram of intensifier prototype

The experimental results are shown in figure 11, the output pressure curve of the supercharger is in the form of square wave. The output pressure reaches the peak pressure in a short time, and then the peak pressure is maintained until the end of the pressurization process. When the input pressure are respectively 1.5MPa,2.5MPa,4.5MPa,7MPa,12MPa, the output pressure are 5.2MPa,10.3MPa, 17.25MPa,29.5MPa, and 52.75MPa, and its pressurization ratio is about equal to the area ratio of the pressurization chamber, the output pressure characteristics of the experimental results are consistent with the numerical simulation results.

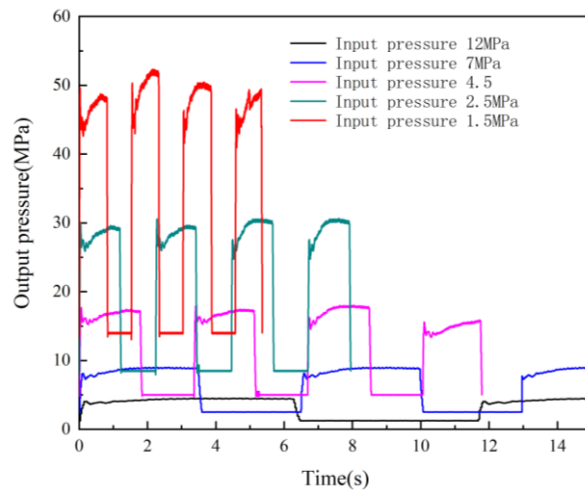


Figure.11 Laboratory test curve of intensifier output characteristics

CONCLUSIONS

In view of the three characteristics of high stress, high strength and high abrasiveness of deep geothermal resources, a method of using ultra-high pressure jet to cut the rock at the bottom of the well and realize local stress unloading is proposed, which can improve the mining efficiency of deep geothermal resources.

The new valve stem downhole intensifier was directly driven by drilling hydraulic power, has simple structure and high energy utilization rate. The greater the ratio of the input pressure to the piston area of the pressurizing chamber and the greater the output pressure, and the faster the working frequency of the intensifier. Increasing the stroke of the pressurizing chamber can increase the holding time of the peak pressure. Compared with the traditional down-hole intensifier, the output Jet features of the new intensifier has a stable period of high-pressure water jet, which is more conducive to rock breaking.

The laboratory test results show that the supercharger is reliable in movement and the supercharging principle is feasible; The output pressure waveform of the supercharger is square wave, and the area ratio of the supercharger chamber is approximately equal to its supercharger ratio; When the input pressure is 2MPa, the output pressure is 9MPa. When the input pressure is 3.5MPa, the output pressure is 14MPa. The experimental test results are consistent with the numerical simulation results.

REFERENCES

- [1] Edoardo R, Shahin J, Volker W, Martin O, Saar, Philipp R. A combined thermo-mechanical drilling technology for deep geothermal and hard rock reservoirs. *Geothermics* 2020;85:101771.
- [2] Moore J, Simmons S. More power from below. *Science* 2013;340(6135):933–934.
- [3] Ma W, Wang Y, Wu X, Liu G. Hot dry rock (HDR) hydraulic fracturing propagation and impact factors assessment via sensitivity indicator. *Renew. Energy* 2020;146:2716–2723.
- [4] Chong Z, Yang S, Babu P, Linga P, Li X. Review of natural gas hydrates as an energy resource: Prospects and challenges. *Appl Energy* 2016;162:1633–1652.
- [5] Ong Y, Lee T J, Jeon J, et al. Background and progress of the Korean EGS Pilot Project World. In: *Proceedings of World Geothermal Congress 2015*. Melbourne: International Geothermal Association, 2015
- [6] Ausse J, Genter A. Types of permeable fractures in granite. *Geol Soc London Spec Publ*, 2005, 240: 1–14.
- [7] Wang M D, Guo Q H, Yan W D, et al. Medium-low-enthalpy geothermal power-electricity generation at Gonghe Basin, Qinghai Province (in Chinese). *Earth Sci-J China Univ Geosci*, 2014, 9: 1317–1322.
- [8] Heng K Y, Chen Z H. Hot dry rock development in China: A long way to go (in Chinese). *Sino-Glob Energ*, 2017, 22: 21–25.
- [9] Duey R. *Smith Bits*, A Schlumberger Company: Axebled ridged diamond element bit [J]. E & P: A Hart Energy Publication, 2017.
- [10] Veenhuizen S D, Kollé J J, Rice C C, et al. Ultra-High Pressure Jet Assist of Mechanical Drilling[C]// *SPE/IADC Drilling Conference*. 1997.
- [11] Liao H, Guan Z, Shi Y, et al. Field tests and applicability of downhole pressurized jet assisted drilling techniques[J]. *International Journal of Rock Mechanics and Mining Sciences*, 2015, 75:140-146.
- [12] Xue L, Li B, Wang Z, et al. Ultrahigh-Pressure-Jet-Assisted Drilling Technique: Theory and Experiment[J]. *Journal of Canadian Petroleum Technology*, 2012, 51(4):276-282.
- [13] Yi X, Zhou C, Liu Y, et al. principle and design of screw downhole supercharger [J]. *Drilling & Production Technology*, 2011.
- [14] Zhao J, B Y J, Sun P, et al. Design of Downhole Supercharger of Double Helical Slots Driven by Screw Motor[J]. *Oil Field Equipment*, 2010.

He, Liao, Sellami, Latham, Xiang, Gerbaud

- [15] Ai C, Zhou R X, Wang Z X, et al. Whole structural design of the diaphragm pressure converter used in bottom hole[J]. Journal of Daqing Petroleum Institute, 2001.
- [16] Jian Z, Zhang G, Xu Y, et al. Enhancing rate of penetration in a tight formation with high-pressure water jet (HPWJ) via a downhole pressurized drilling tool[J]. Journal of Petroleum Science and Engineering, 2018, 174.